

Department of Electronic & Telecommunication
Engineering University of Moratuwa



BM4151 – Biosignal Processing

MATLAB Assignment 3

Continuous and Discrete Wavelet Transforms

Palihakkara A.T. 170418E

This report is submitted in partial fulfillment of the requirements
for the module BM4151 Biosignal processing.

08 November 2021

List of Figures

Figure 1: Daughter wavelets of Mexican Hat Wavelet for several scaling factors	6
Figure 2: Mean & Energy of the Daughter Wavelets	6
Figure 3: Frequency Spectra of the daughter wavelets	7
Figure 4: $x(n)$ Signal	8
Figure 5: Spectrogram of the derived coefficients	8
Figure 6: $X1[n]$ Signal	9
Figure 7: $X2[n]$ Signal	10
Figure 8: $Y1[n]$ - Noisy $X1[n]$ signal.....	10
Figure 9: $Y2[n]$ - Noisy $X2[n]$ signal.....	11
Figure 10: Wavelet function and Scaling function of Haar Wavelet	11
Figure 11: Wavelet function and Scaling function of db9 Wavelet	12
Figure 12: Wavelet properties from waveletAnalyzer - Haar wavelet.....	12
Figure 13: Wavelet properties from waveletAnalyzer - db9 wavelet.....	13
Figure 14: $Y1[n]$ decomposition using Haar wavelet.....	13
Figure 15: $Y1[n]$ decomposition using db9 wavelet.....	14
Figure 16: $Y2[n]$ decomposition using Haar wavelet.....	14
Figure 17: $Y2[n]$ decomposition using db9 wavelet.....	15
Figure 18: Noisy $X1[n]$ reconstructed using Haar wavelet.....	16
Figure 19: Noisy $X1[n]$ reconstructed using db9 wavelet.....	16
Figure 20: Noisy $X2[n]$ reconstructed using Haar wavelet.....	17
Figure 21: Noisy $X2[n]$ reconstructed using db9 wavelet.....	17
Figure 22: Sorted coefficients of Haar wavelet of noisy $X1[n]$	18
Figure 23: Reconstructed noisy $X1[n]$ with Haar wavelet.....	18
Figure 24: Comparing original and denoised $X1[n]$ with Haar wavelet.....	19
Figure 25: Sorted coefficients of db9 wavelet of noisy $X1[n]$	19
Figure 26: Reconstructed noisy $X1[n]$ with db9 wavelet.....	19
Figure 27: Comparing original and denoised $X1[n]$ with db9 wavelet.....	20
Figure 28: Sorted coefficients of Haar wavelet of noisy $X2[n]$	20
Figure 29: Reconstructed noisy $X2[n]$ with Haar wavelet.....	20
Figure 30: Comparing original and denoised $X2[n]$ with Haar wavelet.....	21
Figure 31: Sorted coefficients of db9 wavelet of noisy $X2[n]$	21
Figure 32: Reconstructed noisy $X2[n]$ with db9 wavelet.....	21
Figure 33: Comparing original and denoised $X2[n]$ with db9 wavelet.....	22
Figure 34: aVR lead ECG signal.....	23
Figure 35: Wavelet Decomposition of aVR lead ECG signal using Haar wavelet	23
Figure 36: Wavelet Decomposition of aVR lead ECG signal using db9 wavelet	24
Figure 37: Sorted coefficients of db9 wavelet of ECG signal	24
Figure 38: Reconstructed ECG signal with db9.....	24
Figure 39: Comparing original and reconstructed ECG signal with db9.....	25
Figure 40: Sorted coefficients of haar wavelet of ECG signal.....	25
Figure 41: Reconstructed ECG signal with haar.....	25
Figure 42: Comparing original and reconstructed ECG signal with haar	26

List of Tables

Table 1: Energy comparison between original and reconstructed signals	15
Table 2: Used Thresholds to denoise and the obtained RMSE values	22
Table 3: Compression Ratio Comparison with Haar and db9	26

Wavelet Transform

In the frequency spectrum of a certain signal, Fourier Transform is obtained to get the necessary information about the energy variation of the signal in frequency domain. But it does not include data about the variation of the frequency in time domain.

Wavelet Transform is a method to get all frequency resolution and the time resolution of a given signal.

The continuous wavelet transform equation can be stated as,

$$W(s, \tau) = \int x(t) \frac{1}{\sqrt{s}} \psi\left(\frac{t - \tau}{s}\right) dt$$

Where, s = scaling factor, τ = translation and ψ = wavelet function

In the first part of the assessment is done using the Mexican Hat Wavelet as the continuous wavelet function.

Obtain Mexican Hat function

$$\text{Mexican Hat Fn} = m(t) = -\frac{d^2}{dt^2} g(t)$$

Where,

$$g(t) = \frac{1}{\sqrt{2\pi}} e^{-\frac{1}{2}(t)^2}$$

$$\frac{d}{dt} g(t) = \frac{-t}{\sqrt{2\pi}} e^{-\frac{1}{2}(t)^2}$$

$$\frac{d^2}{dt^2} g(t) = \frac{t^2}{\sqrt{2\pi}} e^{-\frac{1}{2}(t)^2} + \frac{-1}{\sqrt{2\pi}} e^{-\frac{1}{2}(t)^2}$$

$$\therefore m(t) = \frac{(1 - t^2)}{\sqrt{2\pi}} e^{-\frac{1}{2}(t)^2}$$

Calculate the normalizing factor of $m(t)$,

$$E = \int_{-\infty}^{\infty} m(t)^2 dt$$

$$E = \int_{-\infty}^{\infty} \frac{(t^2 - 1)^2 e^{-\frac{t^2}{2}}}{2\pi} dt$$

$$E = \left[\frac{3 \operatorname{erf}(t)}{10\pi} - \frac{t(2t^2 - 1)e^{-t^2}}{81} \right]_{-\infty}^{\infty}$$

$$E = \frac{3}{8\sqrt{\pi}}$$

The energy of Mexican hat function should be equal to 1. Therefore the unity energy can be obtained by normalizing the Mexican hat function.

$$\text{Normalization factor} = \frac{1}{\sqrt{E}} = \sqrt{\frac{8\sqrt{\pi}}{3}}$$

The normalized Mexican hat function can be stated as,

$$m_{\text{normalized}}(t) = \frac{1}{\sqrt{E}} m(t)$$

$$m_{\text{normalized}}(t) = \frac{2\sqrt{2}\pi^{\frac{1}{4}}}{\sqrt{3}} \times \frac{(1-t^2)}{\sqrt{2\pi}} e^{-\frac{1}{2}(t)^2}$$

$$m_{\text{normalized}}(t) = \frac{2(1-t^2)}{\sqrt{3}\pi^{\frac{1}{4}}} e^{-\frac{1}{2}(t)^2}$$

The normalized Mexican hat mother wavelet can be stated as,

$$\psi_{s,\tau}(t) = \frac{1}{\sqrt{s}} \psi\left(\frac{t-\tau}{s}\right)$$

$$\psi_{s,\tau}(t) = \frac{2}{\sqrt{3s}\pi^{\frac{1}{4}}} \left[1 - \left(\frac{t-\tau}{s}\right)^2\right] e^{-\frac{1}{2}\left(\frac{t-\tau}{s}\right)^2}$$

These wavelets have several special properties,

1. Have zero mean
2. Have unity energy
3. Limited in the time domain (Compact Support)

Looking into the function of $m(t)$ we can see that the $m(t)$ is nearly zero for both very large values of t and very small values of t . It implies that, it is a practically time limited signal. Therefore, the Mexican Hat function $m(t)$ has compact support.

Daughter wavelets of the Mexican Hat wavelet obtained for the scaling factors of 0.01 to 2 with 0.1, time intervals are shown in the below Figure 1.

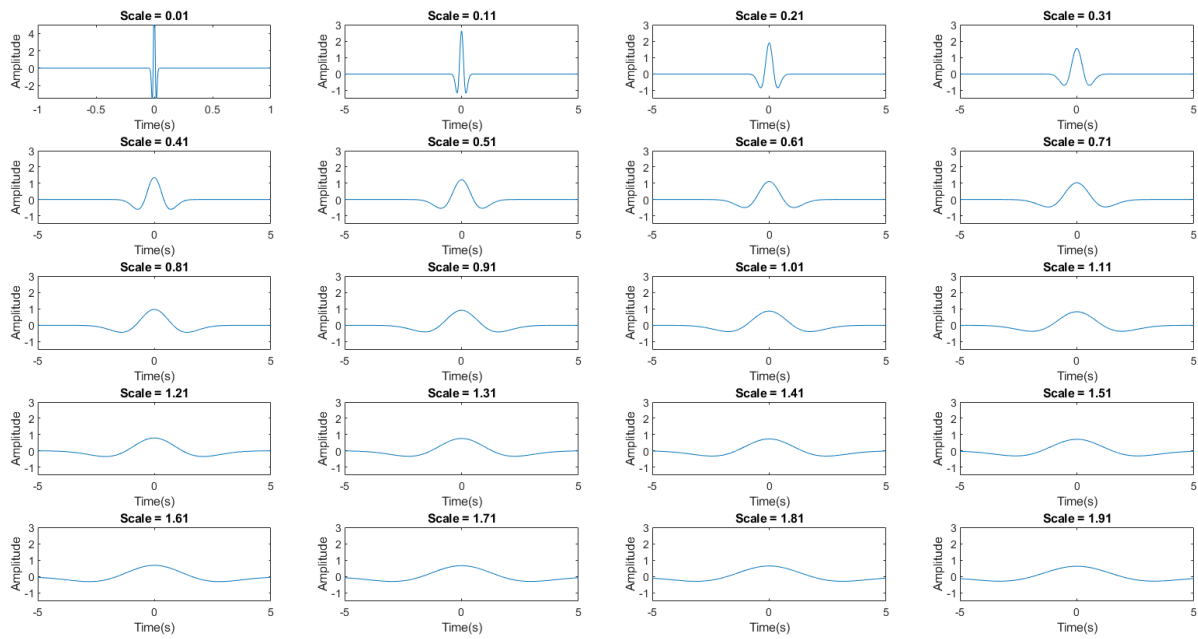


Figure 1: Daughter wavelets of Mexican Hat Wavelet for several scaling factors

According to the Figure 1, we can observe and verify the compact support of the daughter wavelets. All the daughter wavelets of the Mexican Hat wavelet are limited in the time domain as in above Figure 1.

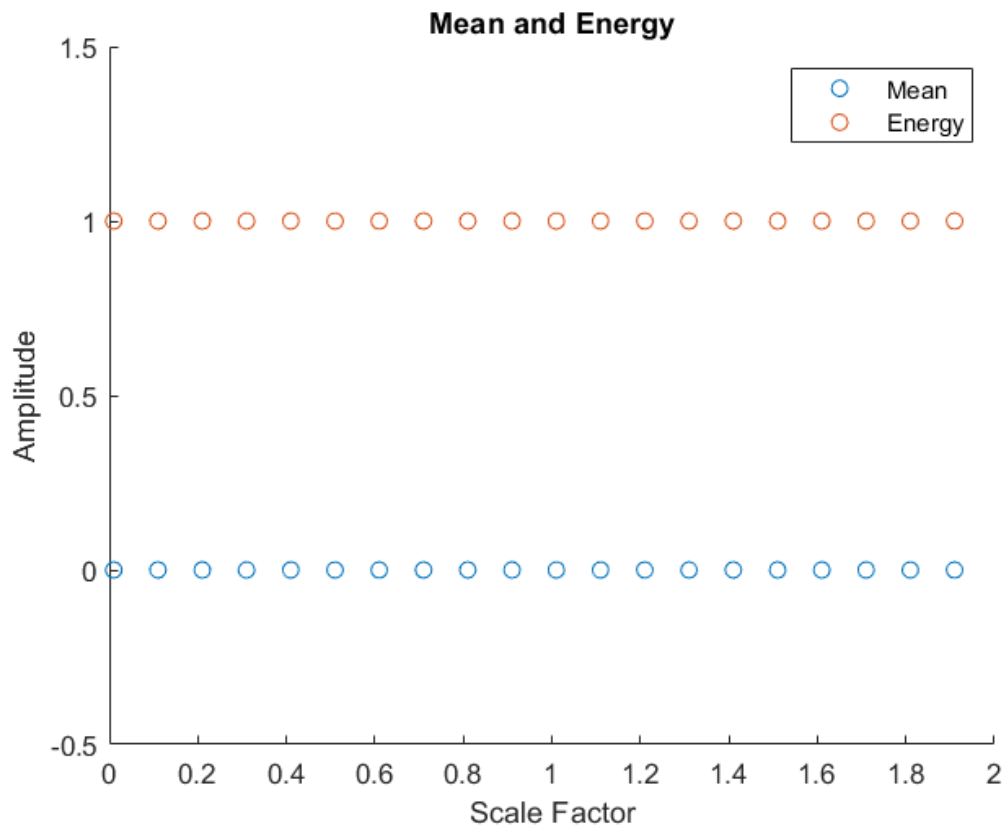


Figure 2: Mean & Energy of the Daughter Wavelets

By looking into the Figure 2, it is shown that the all daughter wavelets have a zero mean and a unity energy as stated above.

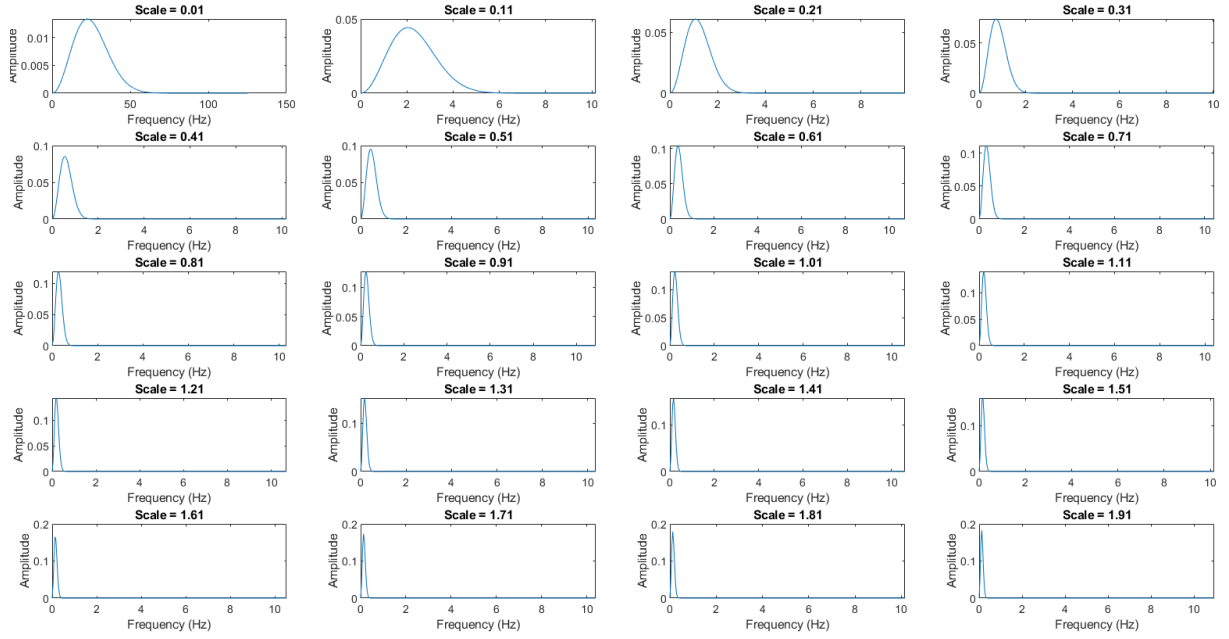


Figure 3: Frequency Spectra of the daughter wavelets

By observing Figure 3, we can say that, in the frequency domain the daughter wavelets have a bandpass characteristic where the center frequency of the pass band depends on the scaling factor. At lower scaling factors, the center frequency is larger, and it decreases with the increasement of the scaling factor. This implies that small scaling factors can capture the high frequency components of the given signal.

Continuous Wavelet Decomposition (CWT)

The continuous signal is obtained using the following equation for the experiment.

$$x(n) = \begin{cases} \sin(0.5\pi n) & 1 \leq n < \frac{3N}{2} \\ \sin(1.5\pi n) & \frac{3N}{2} \leq n < 3N \end{cases}$$

The constructed signal can be shown in the Figure 4.

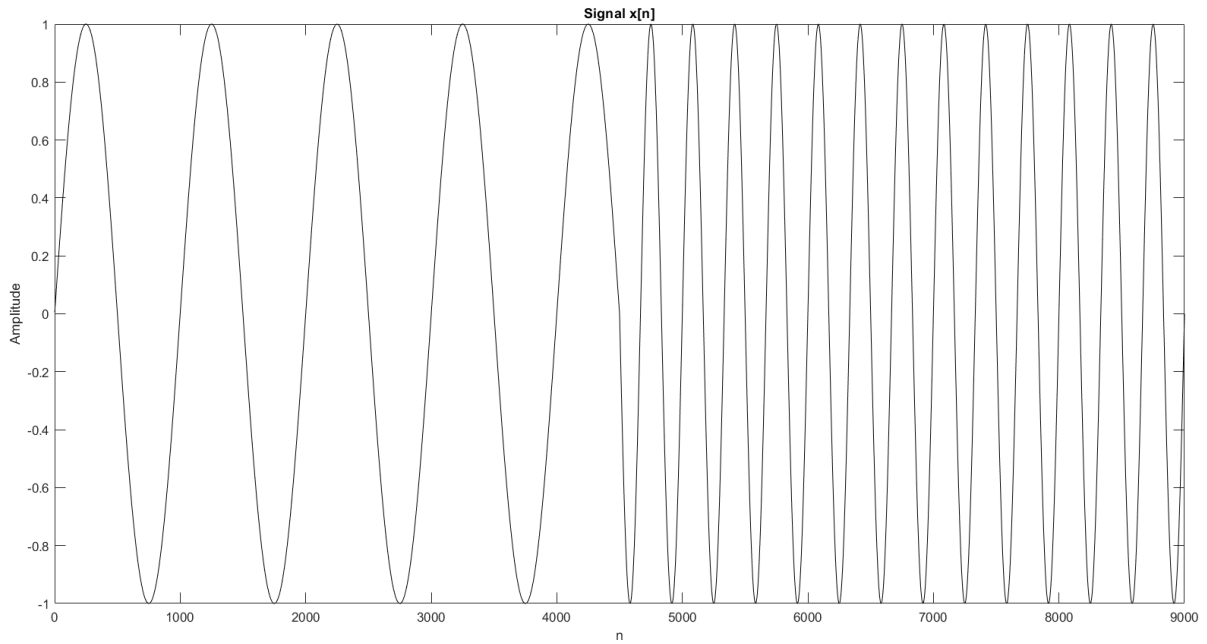


Figure 4: $x(n)$ Signal

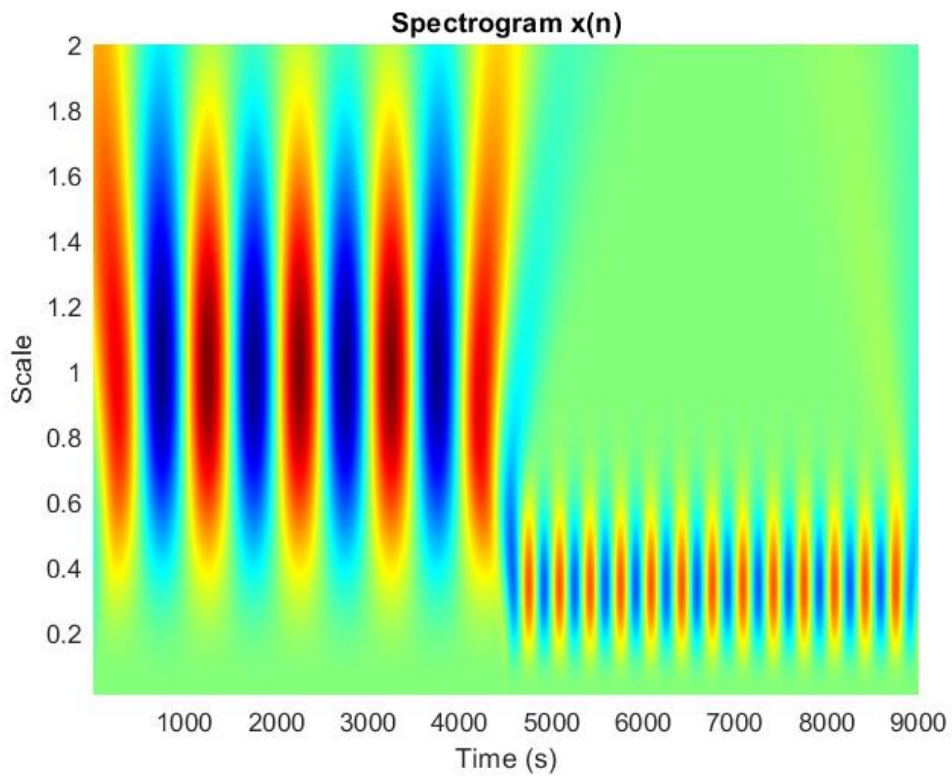


Figure 5: Spectrogram of the derived coefficients

In Figure 3, we observe that the bandwidth of the daughter wavelet reduced with the increasement of the scaling factor. In Figure 5, we can see that the wavelets with higher scaling factors capture the lower frequency part of the signal while the wavelets with lower scaling factors capture the higher frequency part of the signal.

For wavelets with scaling factor near to 1 have the center frequency around $0.5\pi \text{ rads}^{-1}$. As well for wavelets with scaling factor near to 0.32 have the center frequency around $1.5\pi \text{ rads}^{-1}$. Hence the parts of the signal containing those frequencies got highlighted in the spectrogram. Also, we can observe that, for other scaling factors apart from the above two mentioned scaling factors, have low values compared to 1 & 0.31. So, the CWT correctly represents the frequency spectrum and the time domain frequency variation of the signal we derived using the above equation.

Discrete Wavelet Transform (DWT)

A discrete wavelet transform (DWT) decomposes a given signal into a number of sets, where each set is a time series of coefficients describing the time evolution of the signal in the corresponding frequency band. And DWT improves the CWT by getting the discrete scaling factors which reduces the additional computational power and time consumption.

The DWT can be expressed using the following equation,

$$\psi_{m,n}(t) = \frac{1}{\sqrt{S_0^m}} \psi\left(\frac{t - n\tau_0 S_0^m}{S_0^m}\right)$$

Where, $s_0 = \text{scaling step size}$, $\tau_0 = \text{translation step size}$, m & n are corresponding multiplier integers.

And $s_0 = 2, \tau_0 = 1$ are used for the efficient analysis.

For the experiment, we are constructing a sinusoidal signal using the following equation.

$$x_1[n] = \begin{cases} 2 \sin(20\pi n) + \sin(80\pi n) & 0 \leq n < 512 \\ 0.5 \sin(40\pi n) + \sin(60\pi n) & 512 \leq n < 1024 \end{cases}$$

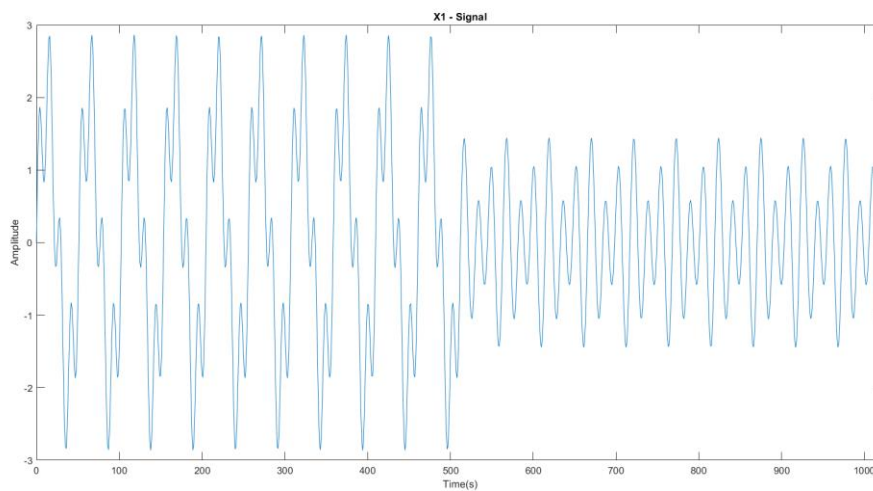


Figure 6: X1[n] Signal

$$x_2[n] = \begin{cases} 1 & 0 \leq n < 64 \\ 2 & 192 \leq n < 256 \\ -1 & 256 \leq n < 512 \\ 3 & 512 \leq n < 704 \\ 1 & 704 \leq n < 960 \\ 0 & \text{otherwise} \end{cases}$$

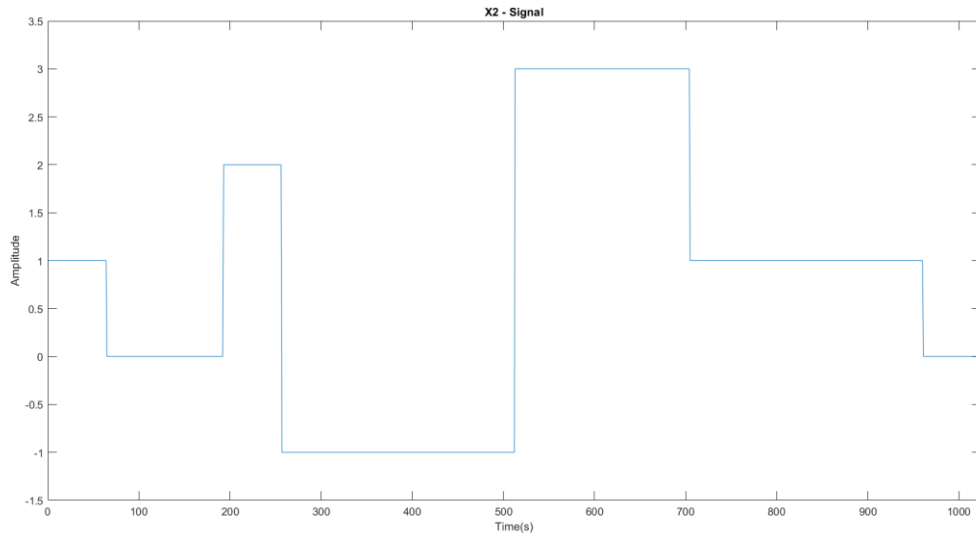


Figure 7: X2[n] Signal

Both signals were corrupted with 10 dB white Gaussian Noise to obtain the noisy signals Y1[n] & Y2[n].

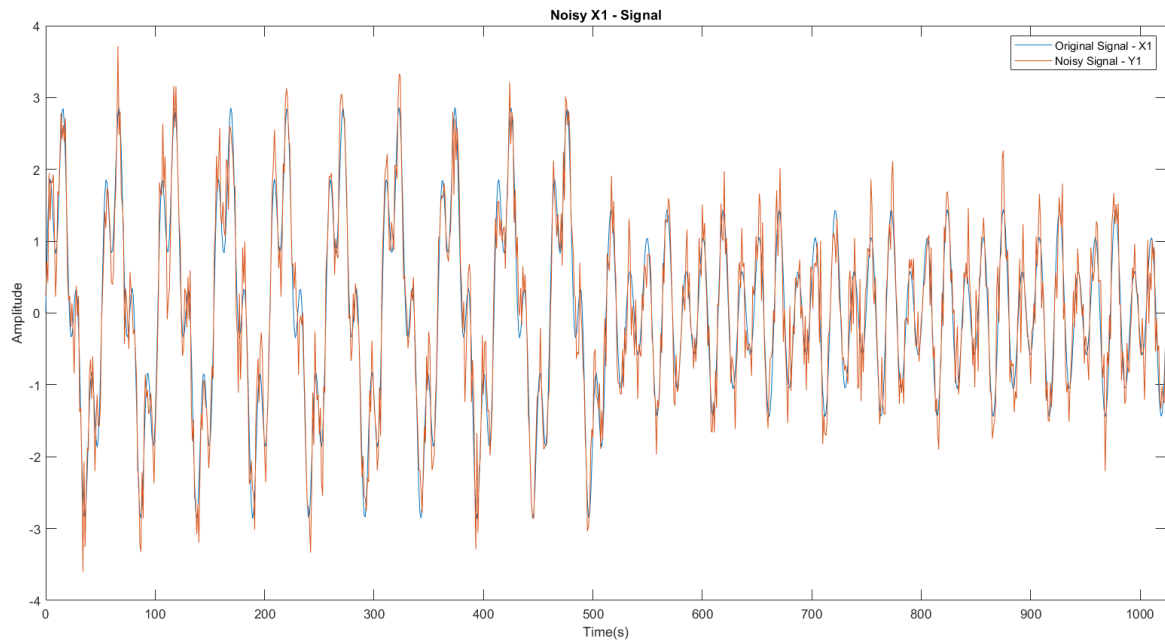


Figure 8: Y1[n] - Noisy X1[n] signal

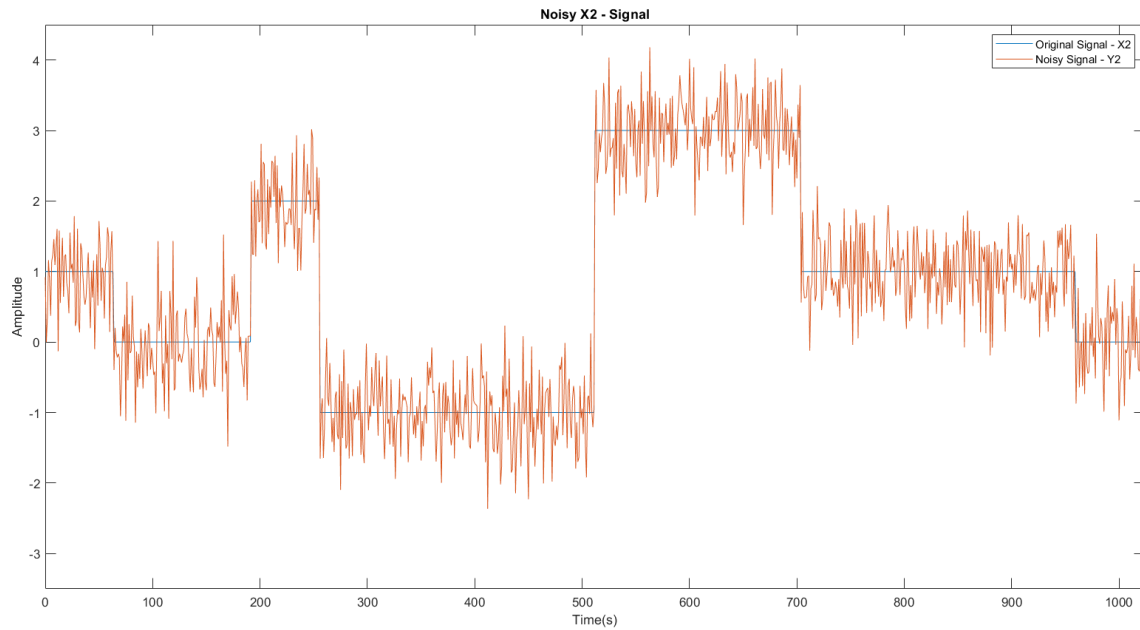


Figure 9: $Y_2[n]$ - Noisy $X_2[n]$ signal

DWT is applied to the above two signals and Haar wavelet and Daubechies 9-tap(db9) wavelet is used as the wavelet functions.

Observing the Wavelets

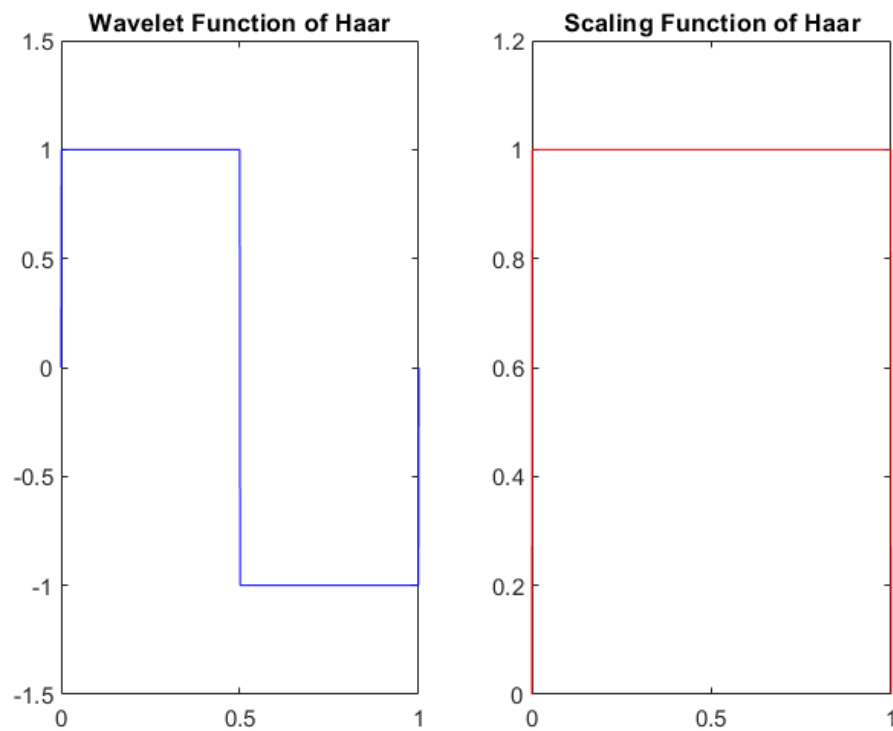


Figure 10: Wavelet function and Scaling function of Haar Wavelet

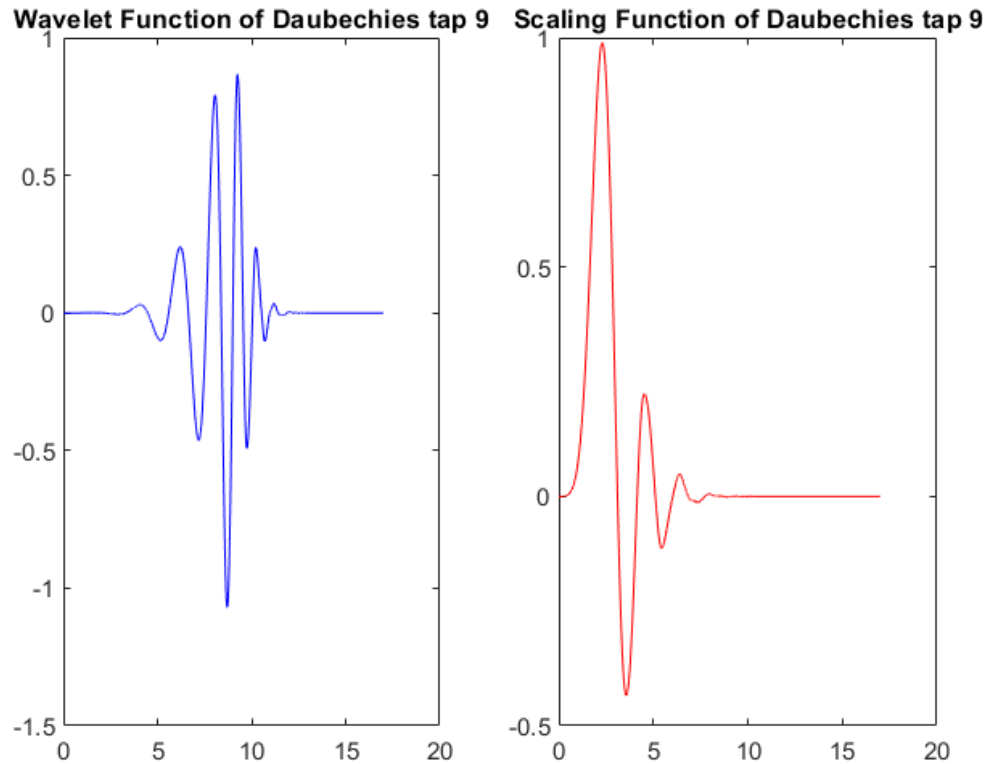


Figure 11: Wavelet function and Scaling function of db9 Wavelet

And the *waveletAnalyzer* tool is used to observe the wavelet properties of haar and db9 wavelets.

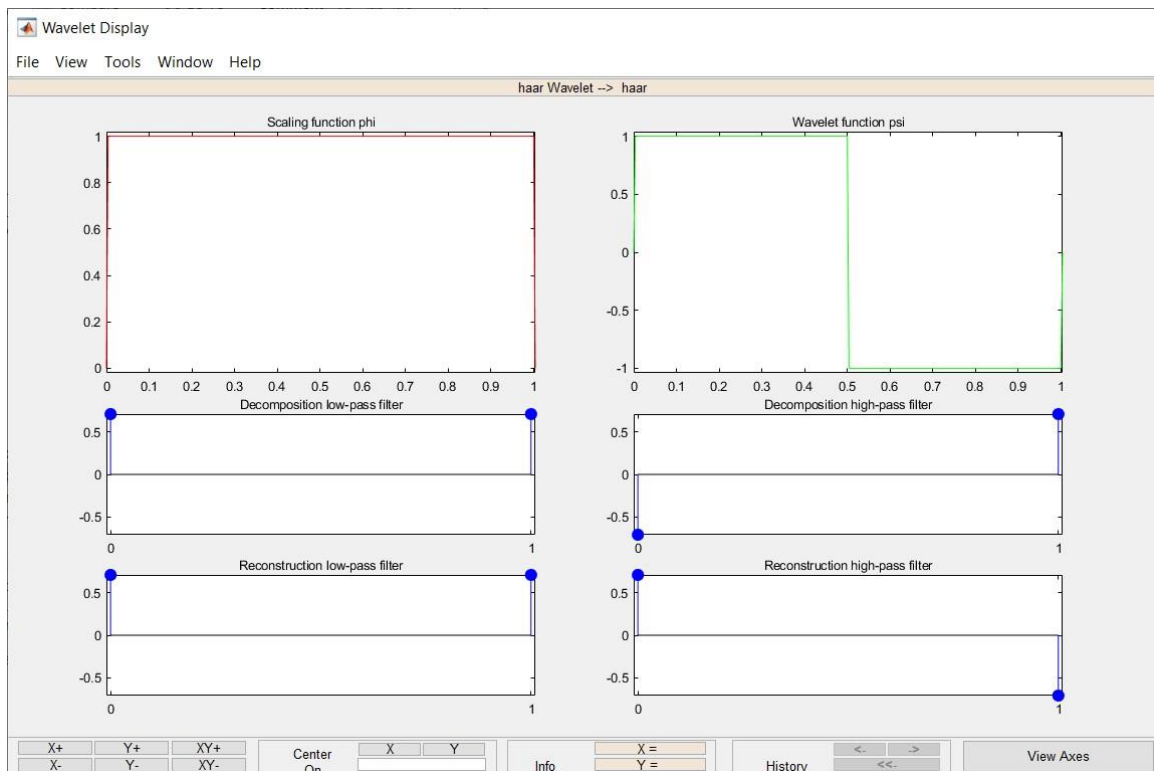


Figure 12: Wavelet properties from waveletAnalyzer - Haar wavelet

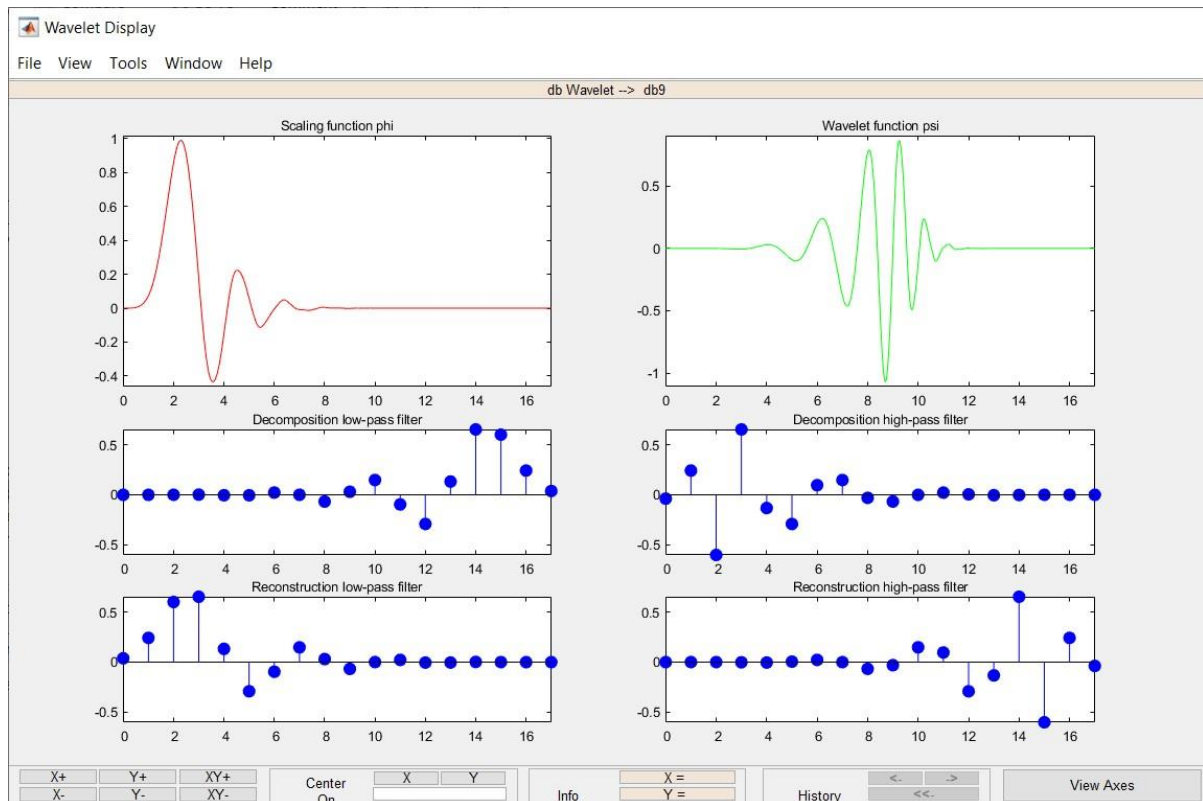


Figure 13: Wavelet properties from waveletAnalyzer - db9 wavelet

Wavelets Decomposition

Since the signal has 1024 samples, the maximum number of dyadic wavelet decompositions can be applied is equal to $\log_2(1024) = 10$

And then the wavelet decomposition is done for the both y1 and y2 noisy signal with haar and db9 wavelets.

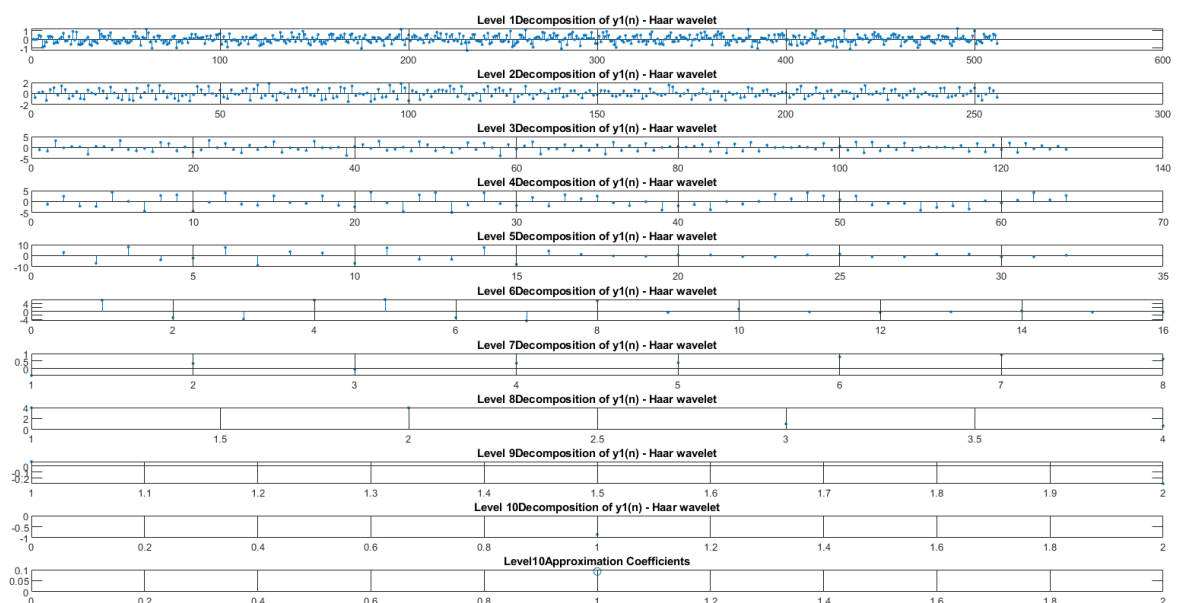


Figure 14: Y1[n] decomposition using Haar wavelet

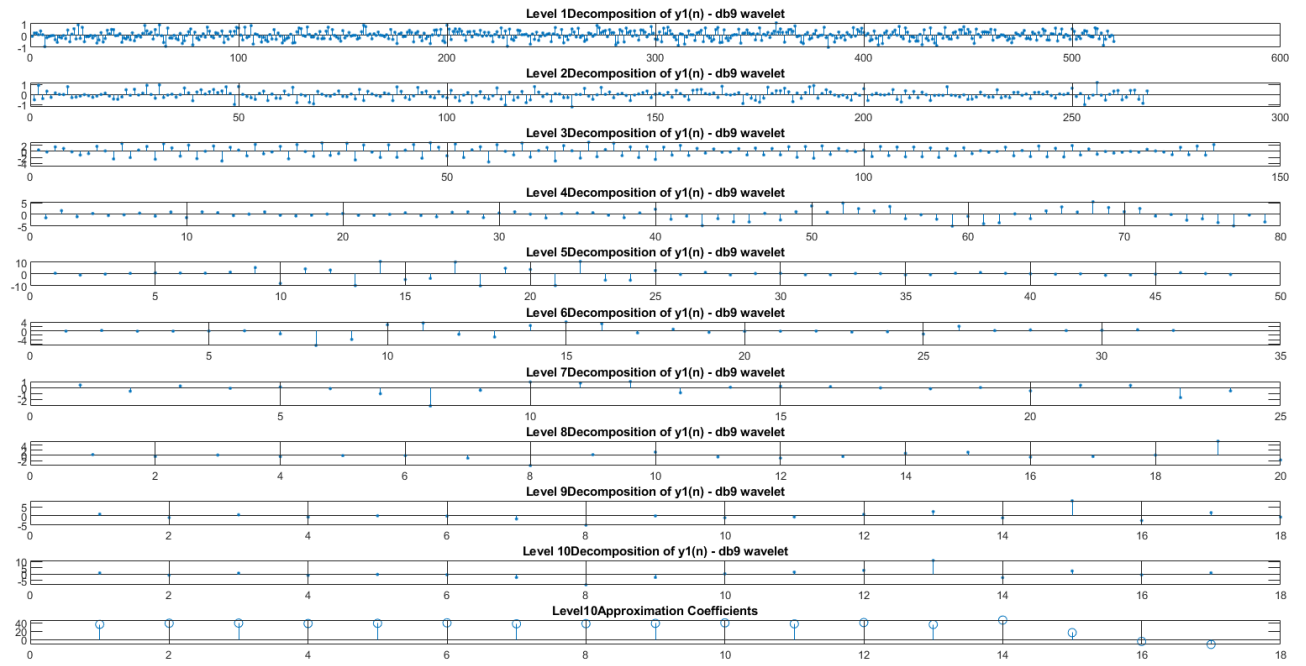


Figure 15: $Y1[n]$ decomposition using db9 wavelet

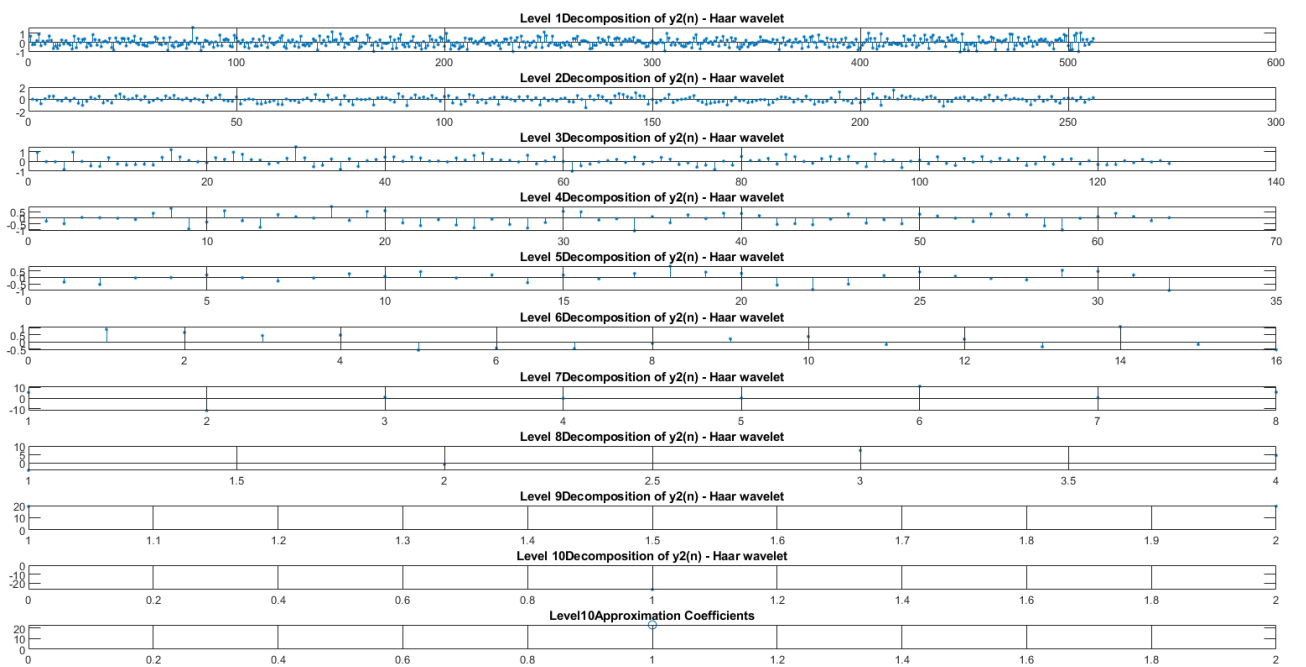


Figure 16: $Y2[n]$ decomposition using Haar wavelet

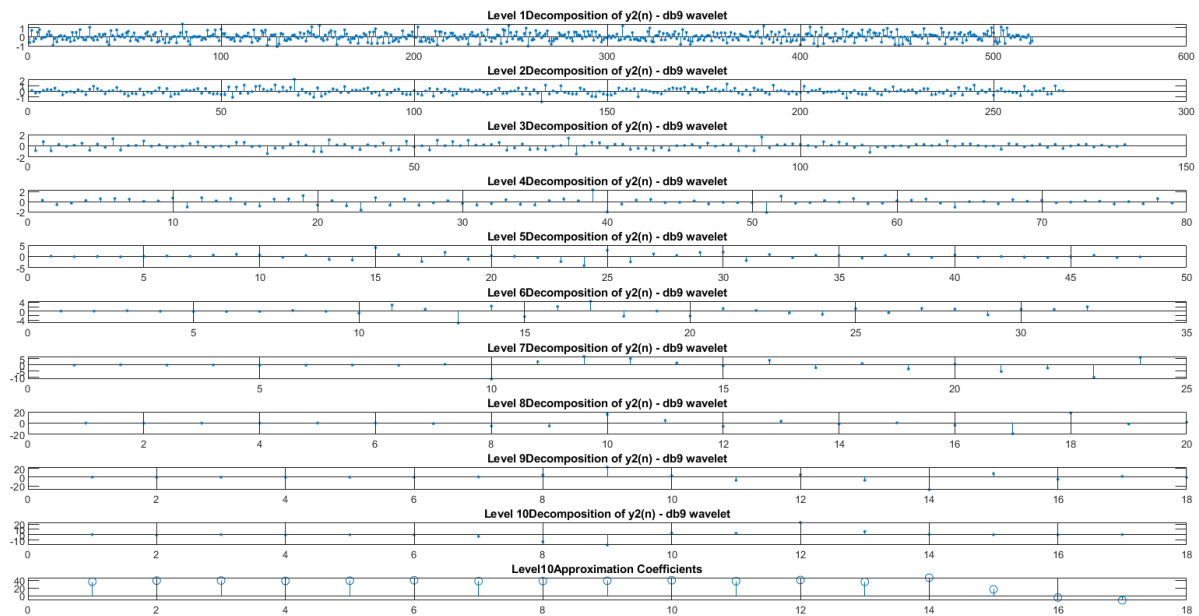


Figure 17: Y2[n] decomposition using db9 wavelet

Table 1: Energy comparison between original and reconstructed signals

	Y1[n]	Y2[n]
Energy of original signal	1716.3488	2781.9525
Energy of Reconstructed with haar wavelet	1716.3488	2781.9525
Energy of Reconstructed X1 with db9 wavelet	1716.3488	2781.9525

Wavelets Reconstruction

The detailed function coefficients and the approximation function coefficient of the respective wavelet according to the number of decomposing levels can be used to reconstruct the signal and verify that the reconstructed and the original signals are identical by comparing the Root mean square error between two signals (RMSE).

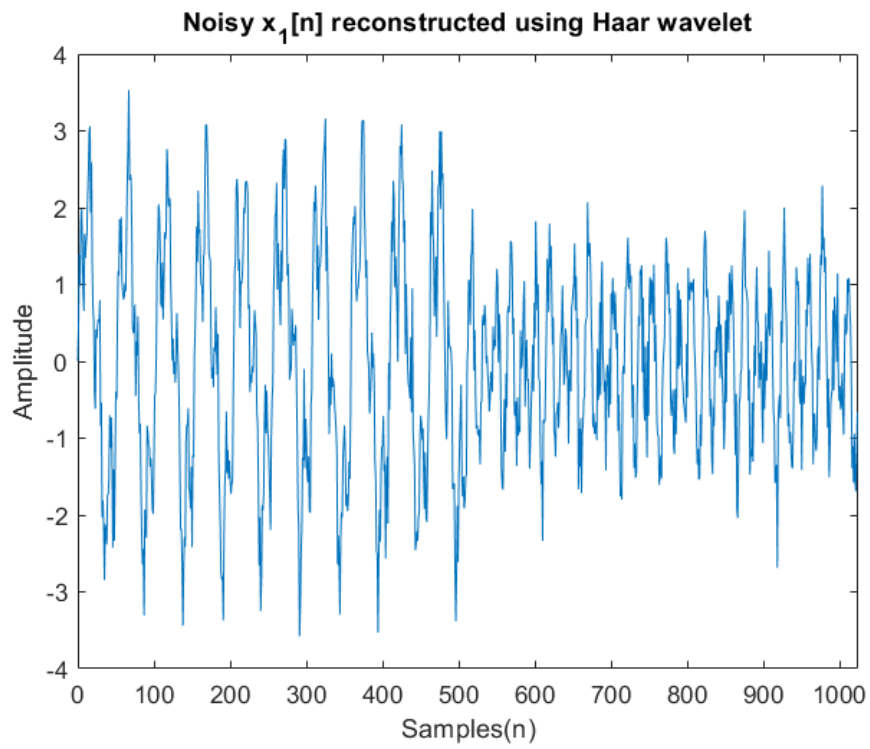


Figure 18: Noisy $x_1[n]$ reconstructed using Haar wavelet

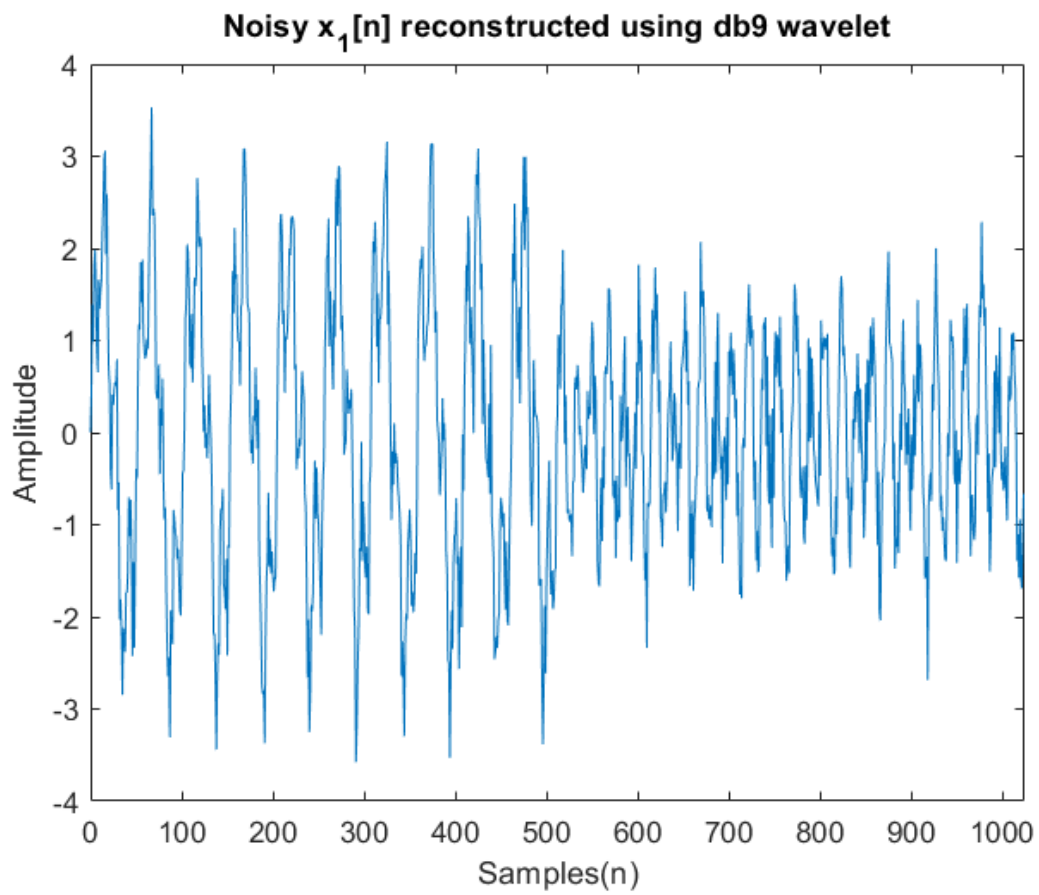


Figure 19: Noisy $x_1[n]$ reconstructed using db9 wavelet

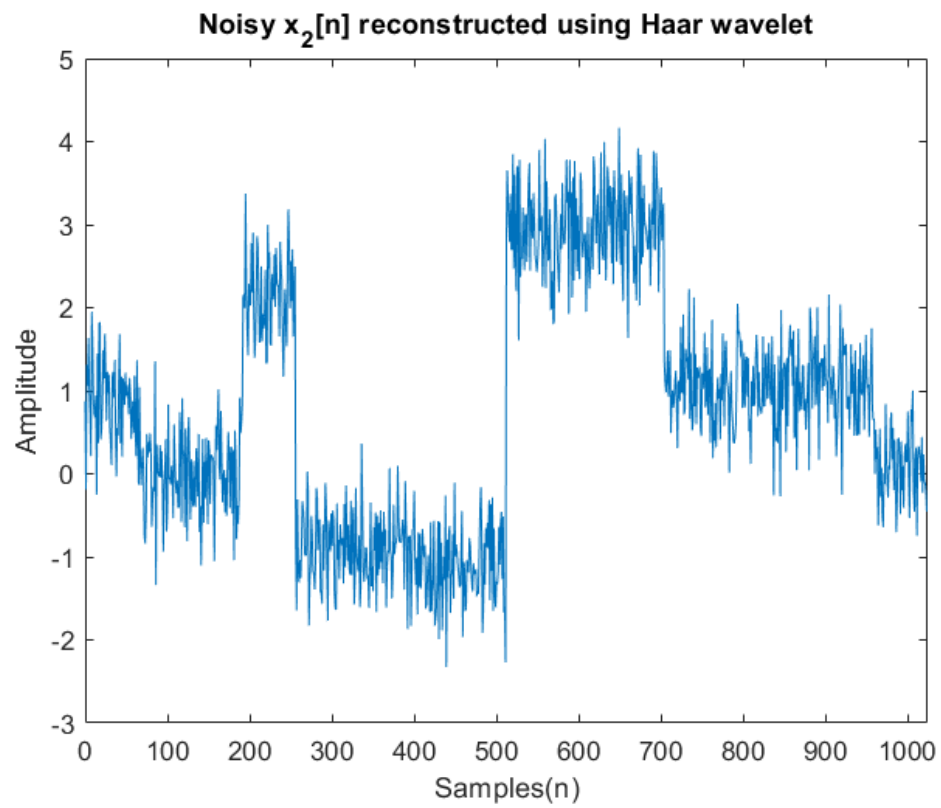


Figure 20: Noisy $x_2[n]$ reconstructed using Haar wavelet

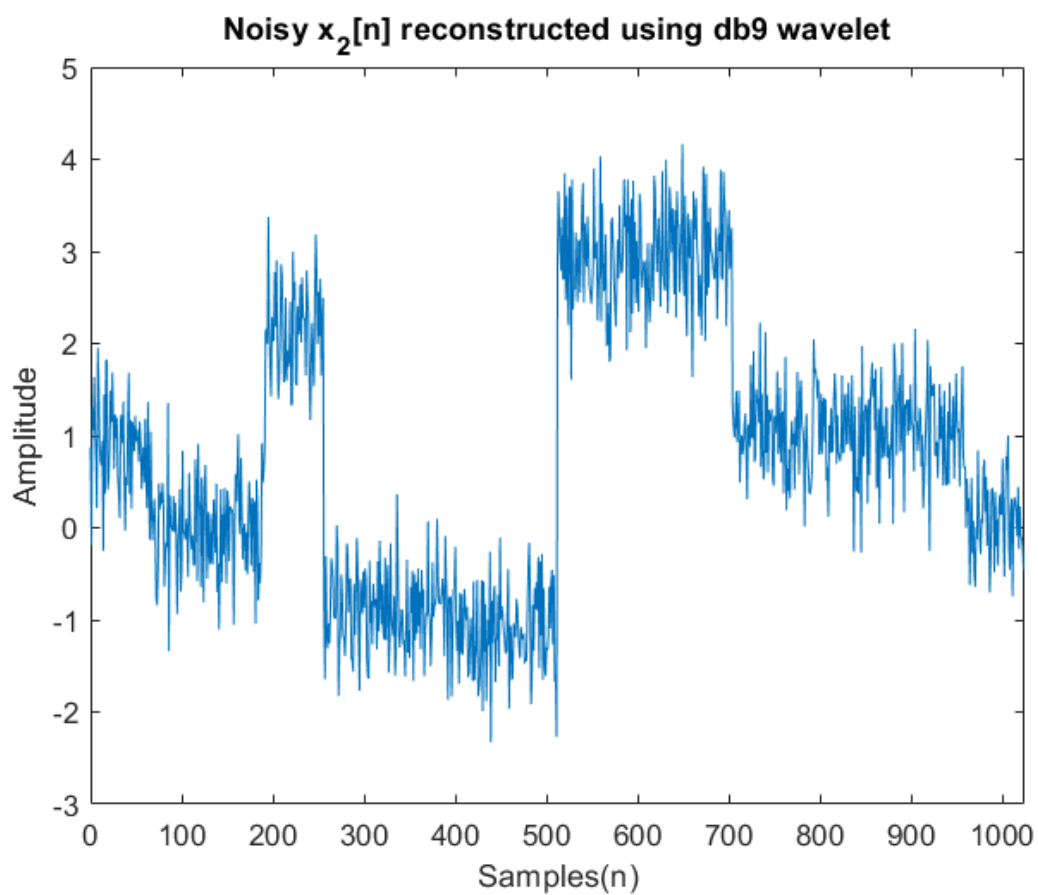


Figure 21: Noisy $x_2[n]$ reconstructed using db9 wavelet

Signal Denoising with DWT

From Wavelet decomposition we can get a set of detailed coefficients at different translations for each scale for the given signal. We can neglect certain features by removing some of the coefficients by setting them to zero and then performing wavelet reconstruction. The removed coefficients are selected using a threshold and coefficient which are lower than the threshold is considered as noise and then removed from the signal.

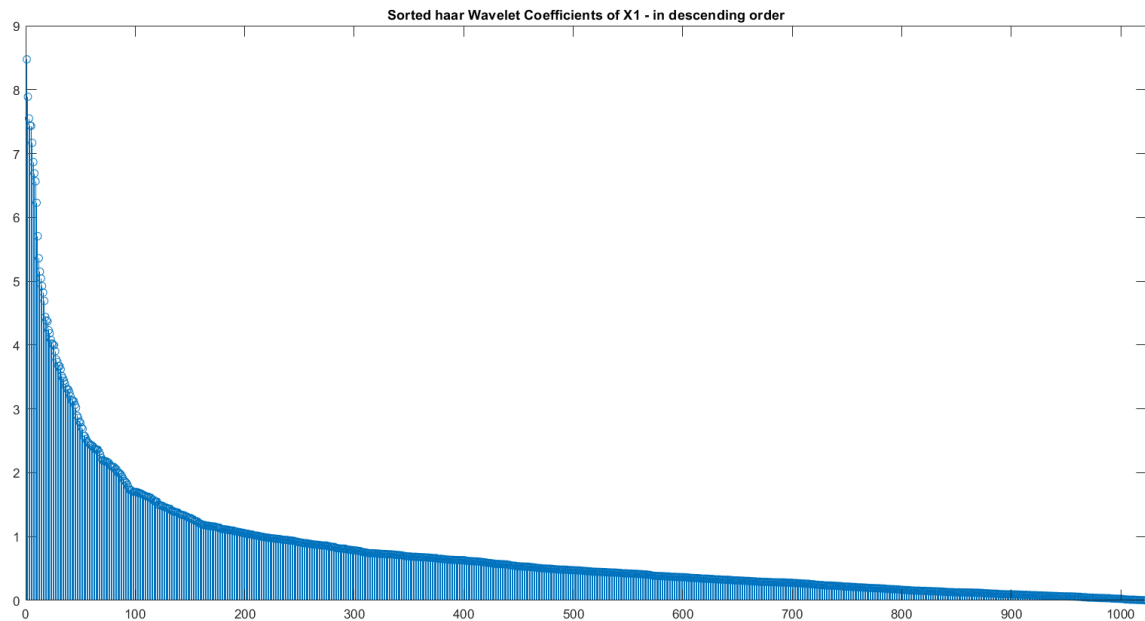


Figure 22: Sorted coefficients of Haar wavelet of noisy $X1[n]$

Observing the coefficients 1 is selected as the threshold for signal denoising.

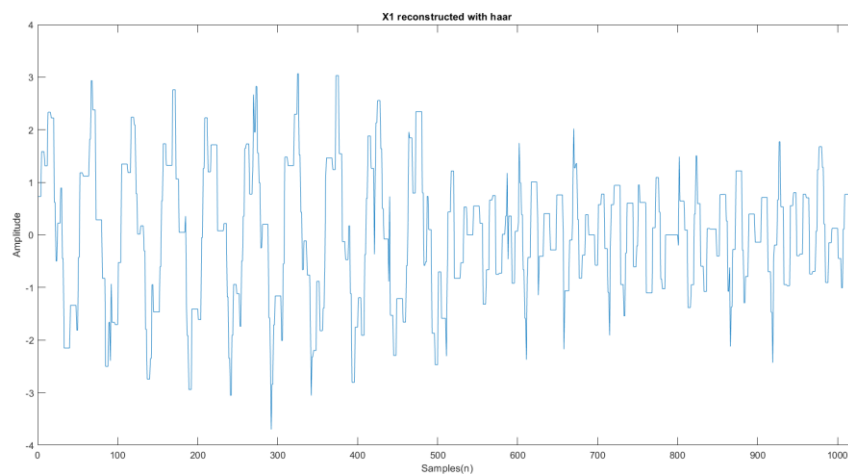


Figure 23: Reconstructed noisy $X1[n]$ with Haar wavelet

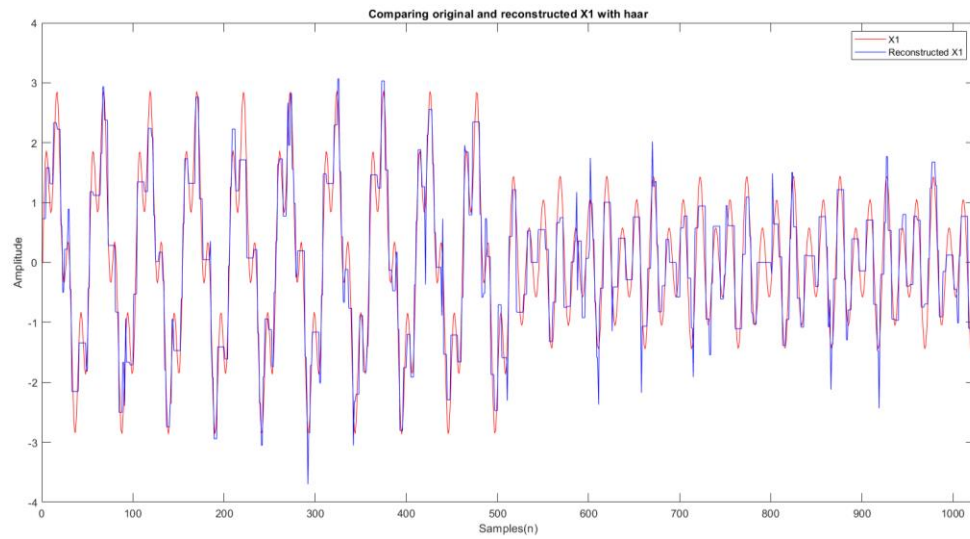


Figure 24: Comparing original and denoised $X1[n]$ with Haar wavelet

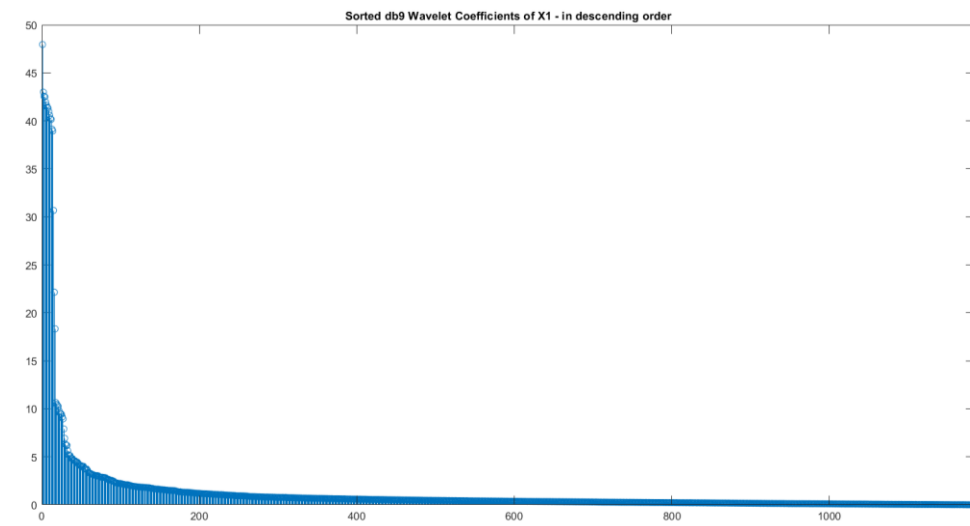


Figure 25: Sorted coefficients of db9 wavelet of noisy $X1[n]$

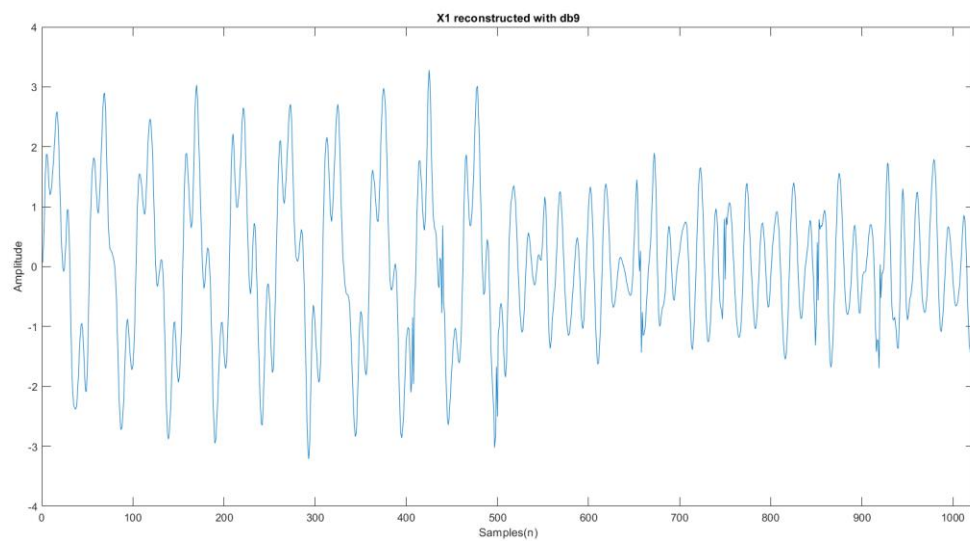


Figure 26: Reconstructed noisy $X1[n]$ with db9 wavelet

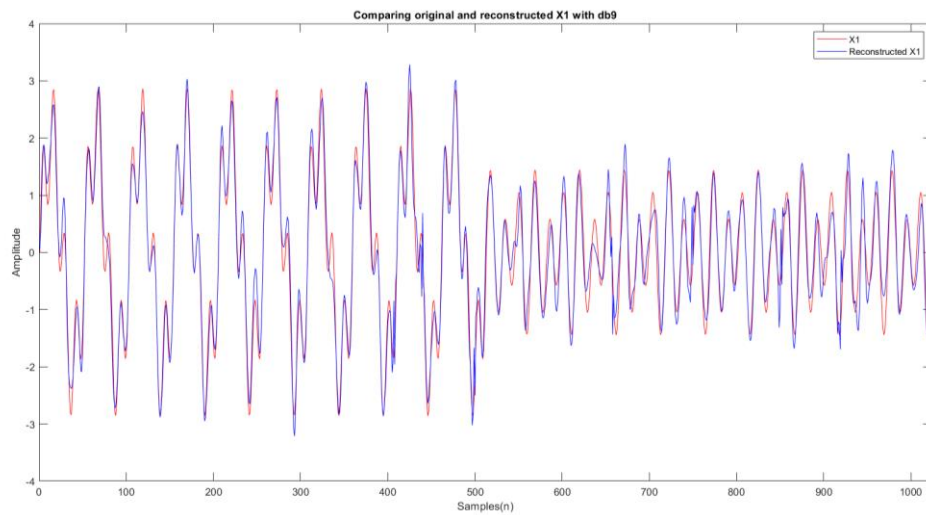


Figure 27: Comparing original and denoised $X1[n]$ with db9 wavelet

Same wavelet transforms were applied to $Y2[n]$ (noisy $X2[n]$) and denoised.

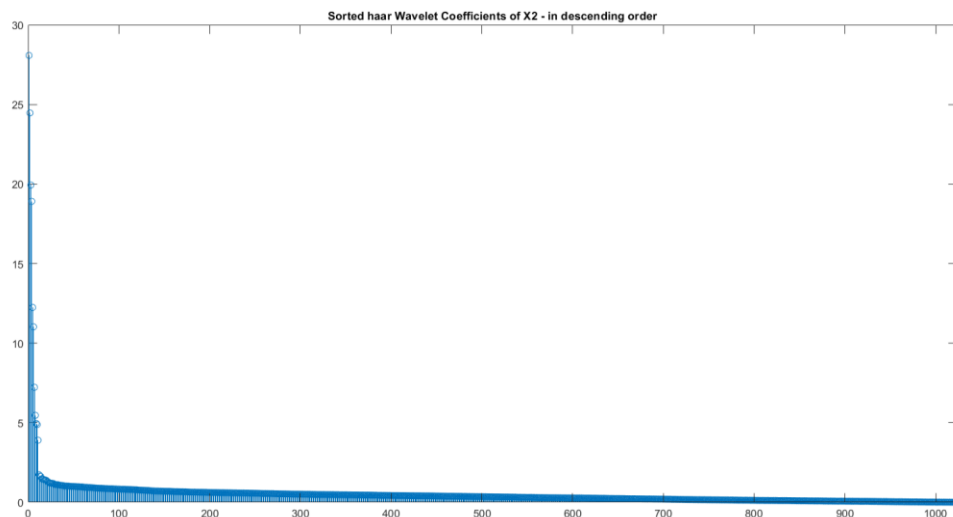


Figure 28: Sorted coefficients of Haar wavelet of noisy $X2[n]$

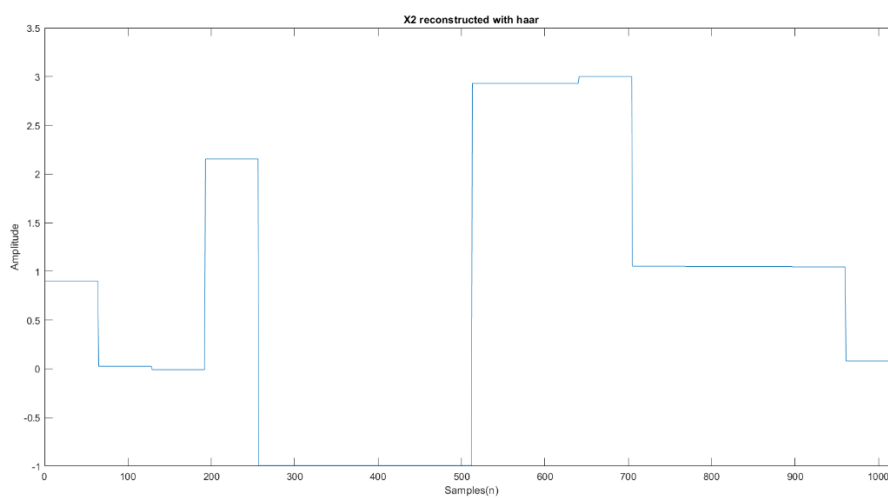


Figure 29: Reconstructed noisy $X2[n]$ with Haar wavelet

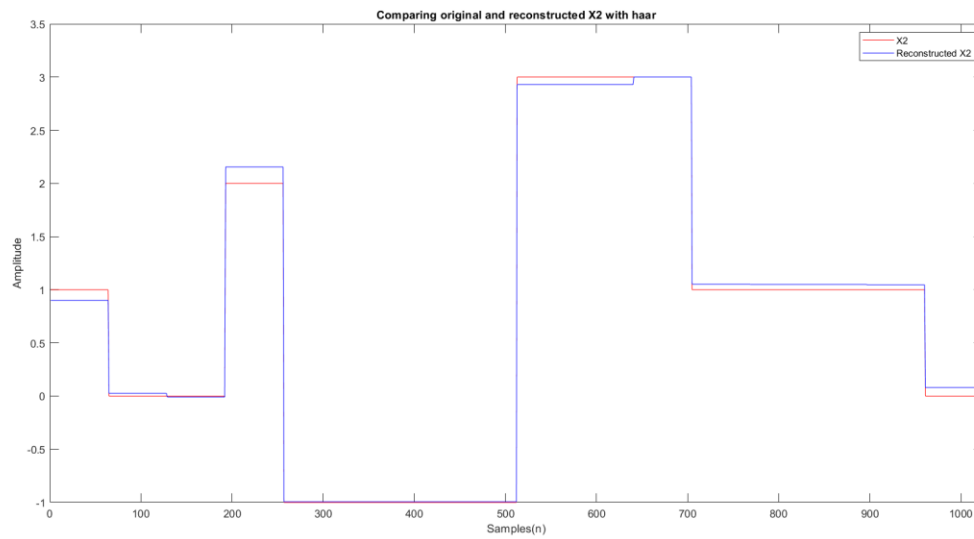


Figure 30: Comparing original and denoised $X2[n]$ with Haar wavelet

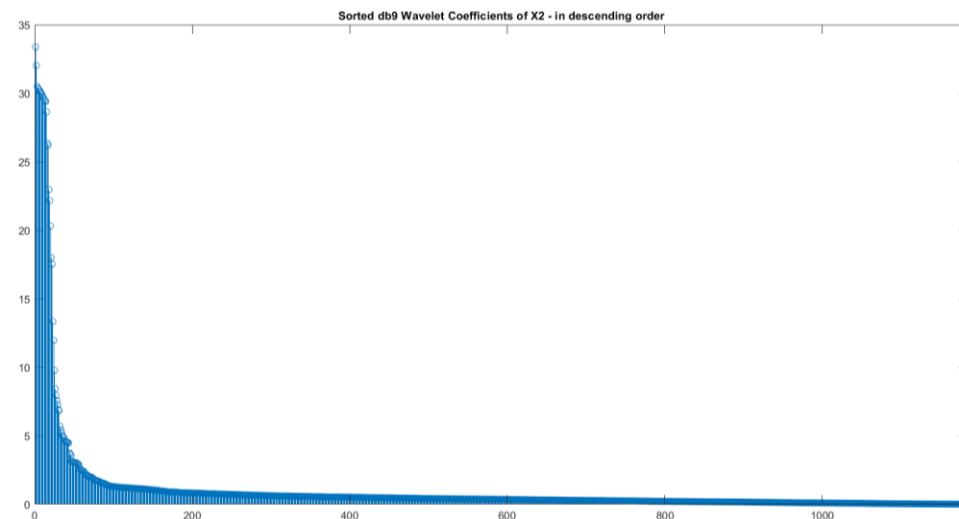


Figure 31: Sorted coefficients of db9 wavelet of noisy $X2[n]$

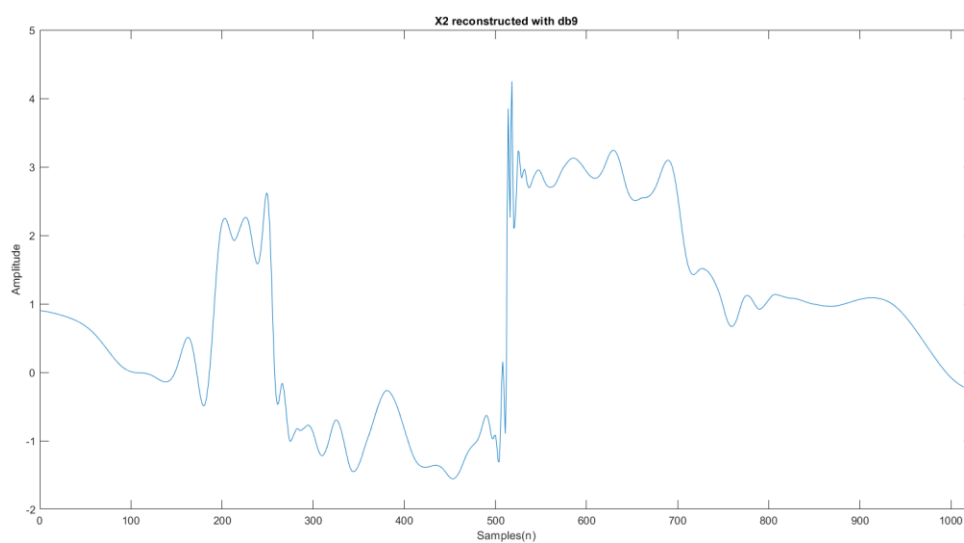


Figure 32: Reconstructed noisy $X2[n]$ with db9 wavelet

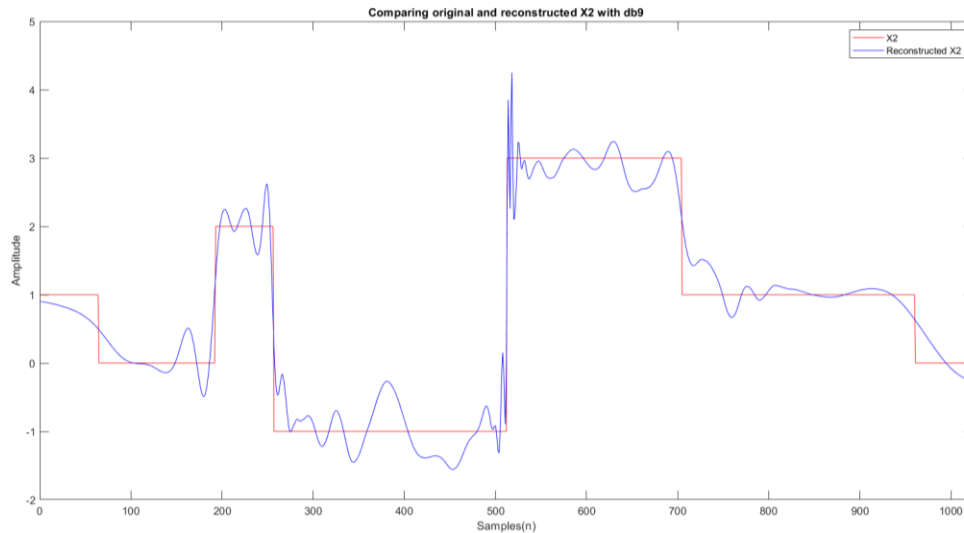


Figure 33: Comparing original and denoised X2[n] with db9 wavelet

Table 2: Used Thresholds to denoise and the obtained RMSE values

Signal	Wavlet	Threshold	RMSE
Y1[n]	Haar	1	0.42121
	db9	1	0.25205
Y2[n]	Haar	2	0.047035
	db9	2	0.30136

The RMSE values for the application of Haar wavelet is lower than when the Daubechies tap-9 wavelet when comparing. The signals with rapid transitions just like Y2[n] can be denoised using the Haar wavelet therefore a better fit can be obtained. As well signals with sinusoidal variations like Y1[n] it can be denoised using the Daubechies tap-9 wavelet is better when comparing the plots and the RMSE values.

Signal Compression with DWT

Wavelet coefficients that are very small can be neglected as they have a minimal contribution to the signal, and they will be considered as the added noise to the original signal. In signal compression wavelet coefficients are kept until those components preserves the given percentage of the energy. Other components are removed by setting them to zero.

For the signal compression aVR lead ECG raw signal with sampling frequency of 257 Hz is loaded and applied the two wavelet transforms.

The maximum number of dyadic wavelet decompositions can be applied is equal to $\log_2(2570) \approx 12$

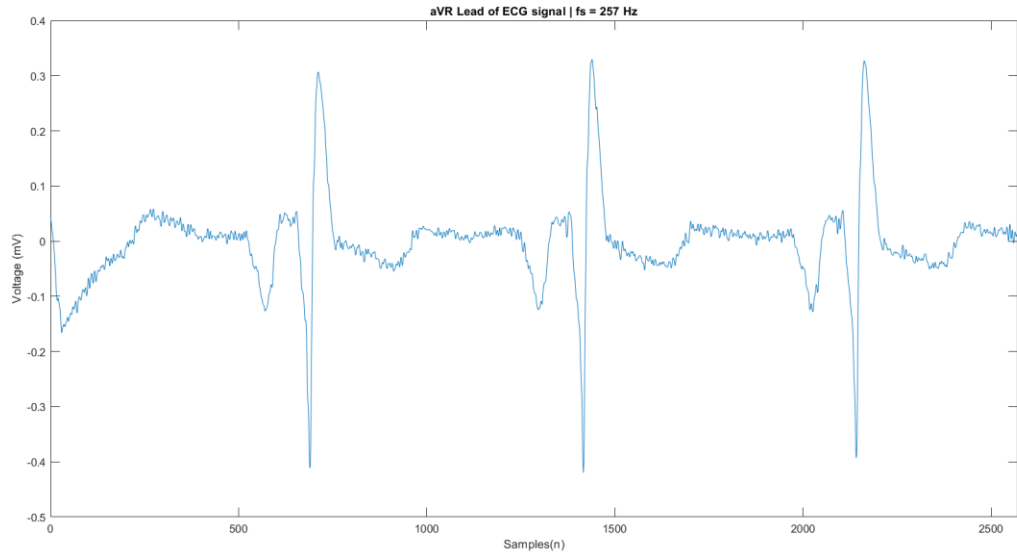


Figure 34: aVR lead ECG signal

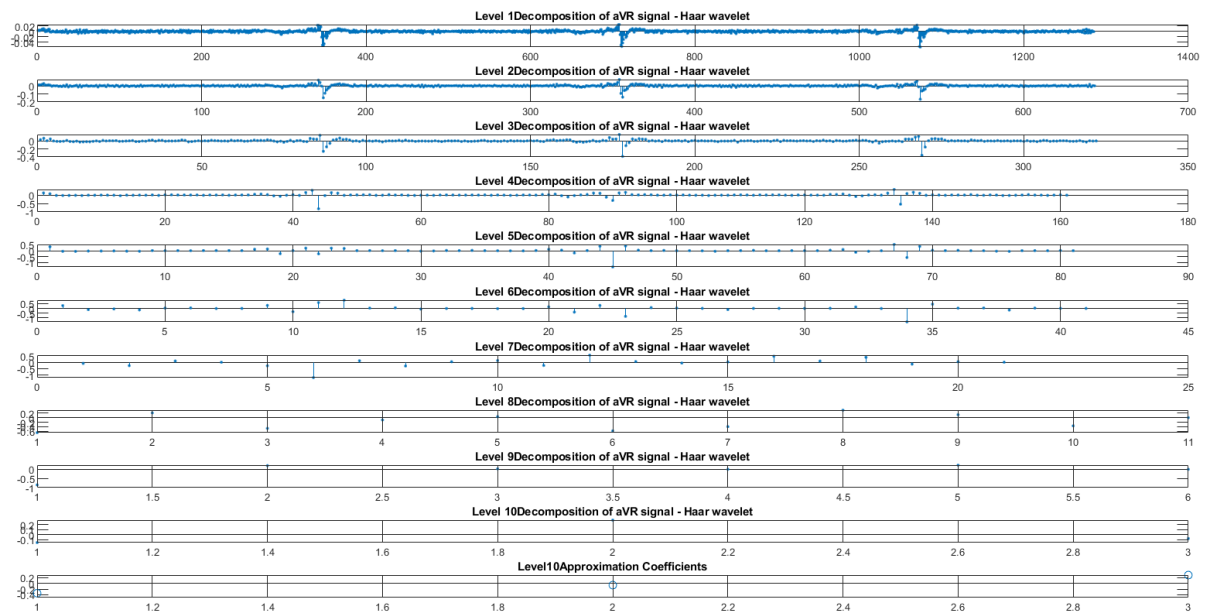


Figure 35: Wavelet Decomposition of aVR lead ECG signal using Haar wavelet

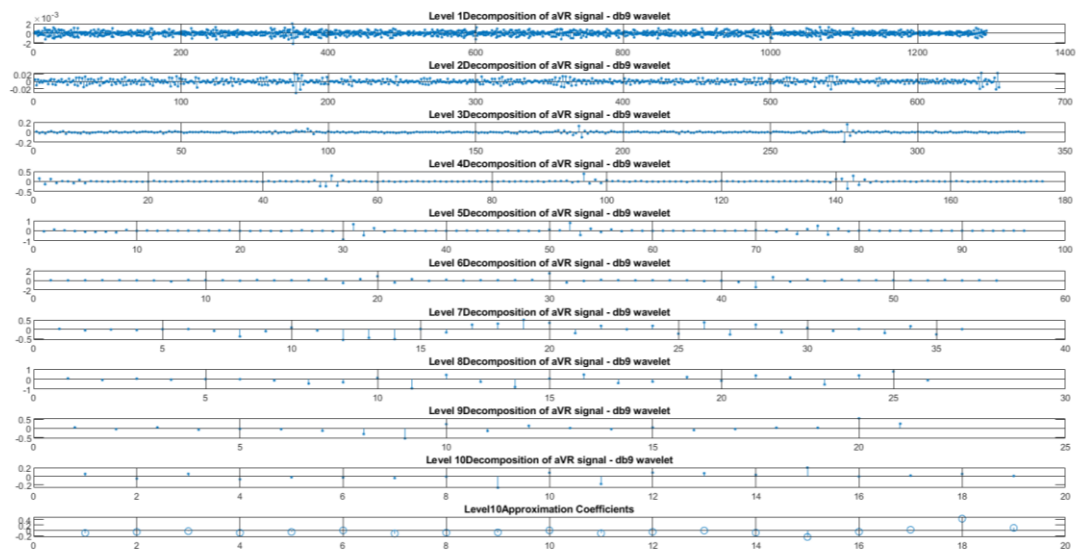


Figure 36: Wavelet Decomposition of aVR lead ECG signal using db9 wavelet

Signal Compression

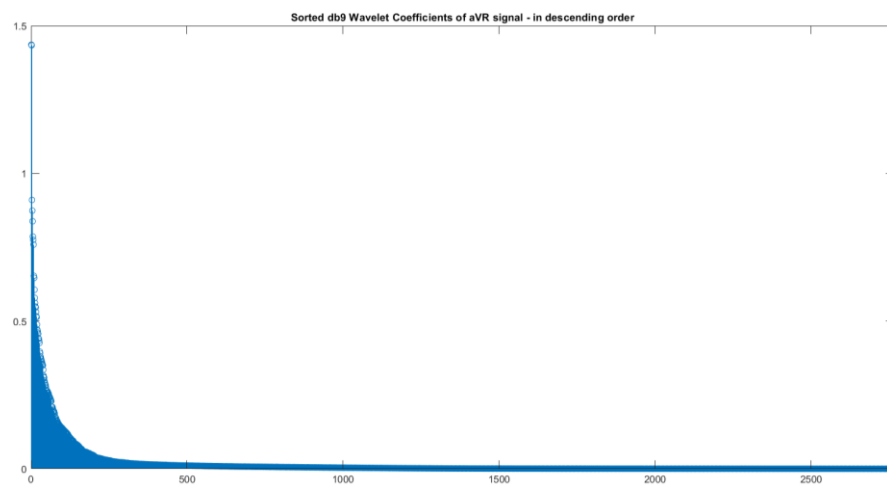


Figure 37: Sorted coefficients of db9 wavelet of ECG signal

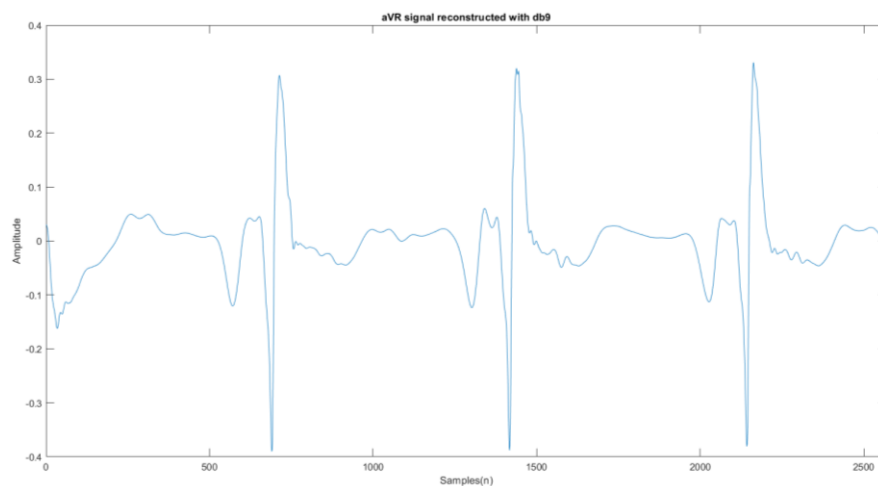


Figure 38: Reconstructed ECG signal with db9

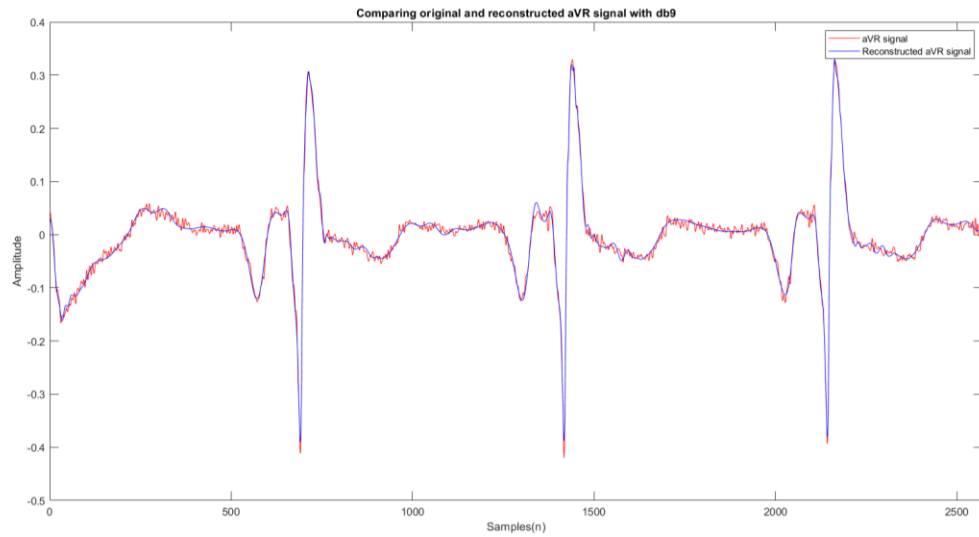


Figure 39: Comparing original and reconstructed ECG signal with db9

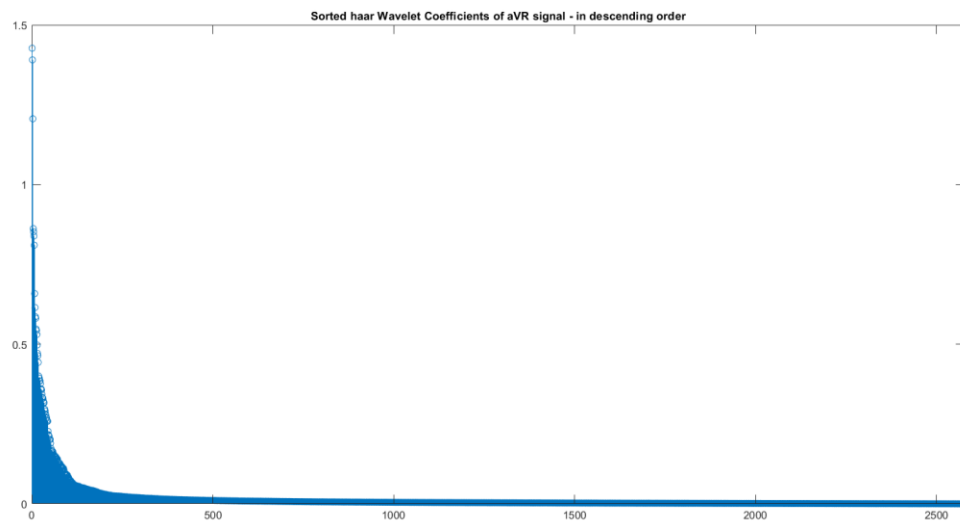


Figure 40: Sorted coefficients of haar wavelet of ECG signal

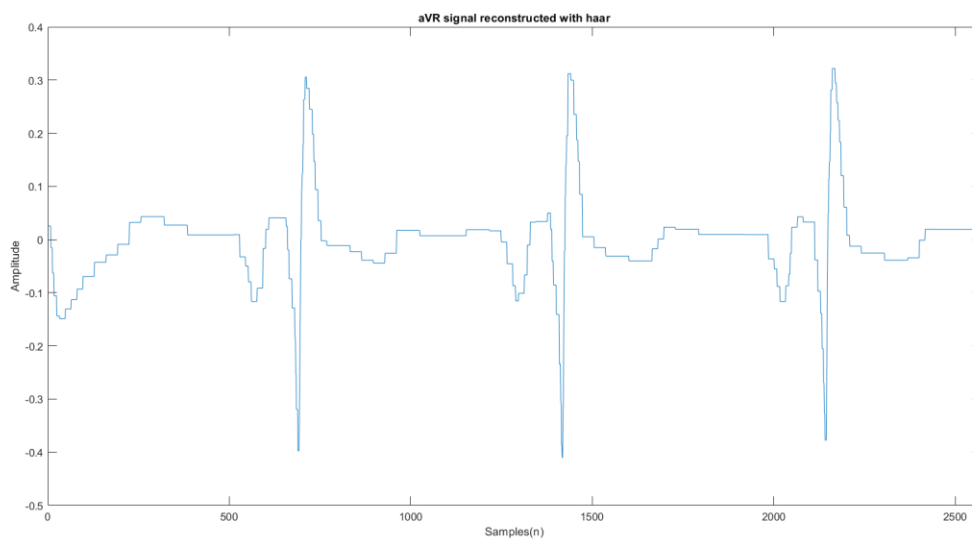


Figure 41: Reconstructed ECG signal with haar

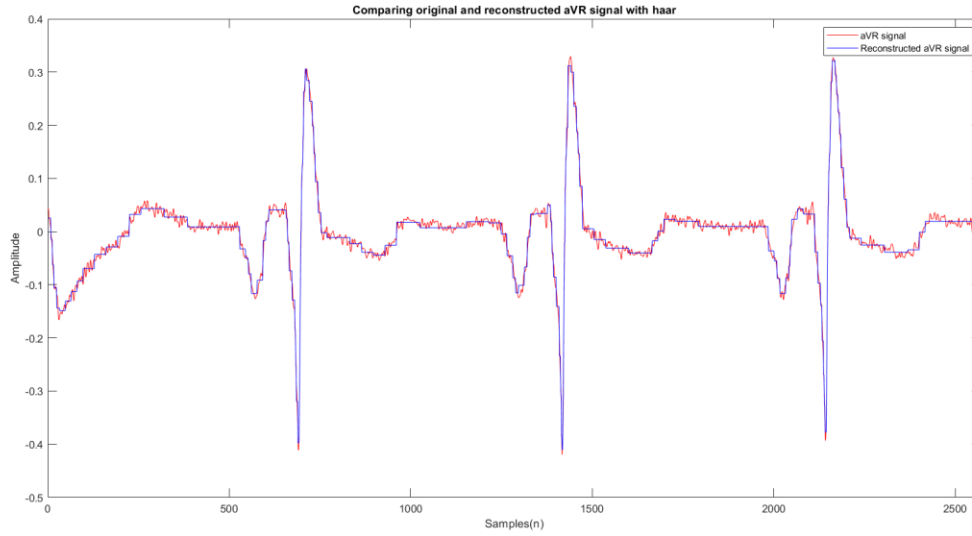


Figure 42: Comparing original and reconstructed ECG signal with haar

Table 3: Compression Ratio Comparison with Haar and db9

Wavelet	Energy Percentage	Compression Ratio	RMSE
Haar	99%	17.1801	6.5711×10^{-5}
Db9	99%	18.6812	9.1811×10^{-5}

$$\text{Compression Ratio} = \text{Signal Length} / \text{Selected signal coefficients}$$

Since the haar wavelet has sharp edges, it is unable to reconstruct the ECG signal properly with the shape. But the db9 wavelet was able to construct the signal well comparing to haar wavelet. And the low RMSE value verifies that fact.